Russian Physics Journal, Vol. 51, No. 9, 2008

METHOD OF ULTRAWIDEBAND RADIO-PULSE LOGGING OF HORIZONTAL WELLS

M. I. Épov,[1] O. V. Yakubova,[2] E. D. Tel'pukhovskii,[2, 3] V. L. Mironov,[3] and V. P. Yakubov[2, 3]

UDC 538.56

Results of measuring the properties of oil-and-gas collector media using ultrawideband (UWB) radio pulses are presented. A new method of pulsed electromagnetic logging is suggested.

INTRODUCTION

A fundamental problem solved in the present work is investigation into the special features of ultrawideband (UWB) pulse propagation in specific media of an oil-and-gas collector. The concrete applied purpose of the work is to study the UWB pulse propagation through model media of the oil-and-gas collector and on this basis, to estimate the possibility of UWB pulse application for logging and navigation of tools for horizontal drilling. Interest in these studies constantly increases all over the world and in Russia [1–5]. It is *a priori* assumed that the use of UWB pulses will allow fairly deep penetration into oil-bearing media with sufficient spatial resolution to be provided. The present work is based on the experimental UWB data and addresses the question as to whether the UWB methods are efficient for radio-pulse logging in the exploitation of hydrocarbon fields.

EXPERIMENTAL STUDY

UWB pulses were generated by three generators produced by the Limited Liability Company TRIM Scientific Production Enterprise (LLC TRIM SPE), Saint Petersburg, including TMG 1500.080R02 and TMG 100.010R01 generators of bipolar pulses and TMG 07501R01 generators of unipolar pulses. The TMG 1500.080R02 generator generates pulses whose waveforms are close to a one-period sinusoid with amplitude of ±80 V. Pulse duration at a level of 0.1 of maximum is 1500 ps, and pulse repetition frequency is 100 kHz. The TMG 100.010R01 generator of bipolar pulses generates pulses whose waveforms are close to a one-period sinusoid, amplitude is ±10 V, pulse duration at a level of 0.1 of maximum is 100 ps, and pulse repetition frequency is 1 MHz. The TMG 07501R01 generator of unipolar pulses has analogous characteristics. Figure 1 shows waveforms and spectra of these pulses. It can be seen that they cover the frequency range from 0.1 to 20 GHz. It is *a priori* obvious that the generator of 1500-ps pulses provides the greatest penetration depth, but the generator of 100-ps pulses is more preferable for obtaining high spatial resolution. Most experiments were performed with it.

To register UWB pulses, a TMR8140 two-channel stroboscopic digital oscillograph was used. This oscillograph produced by the LLC TRIM SPE has the following specifications:

Bandwidth	0–40 GHz
Dynamic range of input signals	±1 V
Time window	0.01–100 ns/div
Sensitivity	5–200 mV/div

[1]Institute of Geophysics and Geology of the Siberian Branch of the Russian Academy of Sciences, Novosibirsk, Russia; [2]Tomsk State University, Russia, e-mail: yvlp@mail.ru; [3]L. V. Kirenskii Institute of Physics of the Siberian Branch of the Russian Academy of Sciences, Krasnoyarsk, Russia. Translated from Izvestiya Vysshikh Uchebnykh Zavedenii, Fizika, No. 9, pp. 63–70, September, 2008. Original article submitted June 10, 2008.

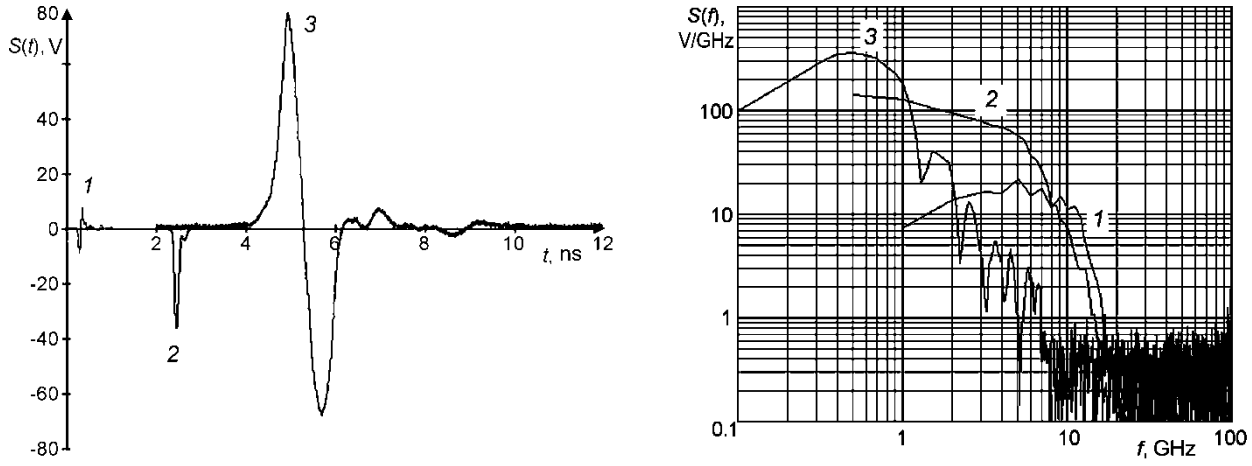

Fig. 1. UWB pulses with duration of 100 (curve *1*), 200 (curve *2*), and 1500 ps (curve *3*) used for probing and their spectra.

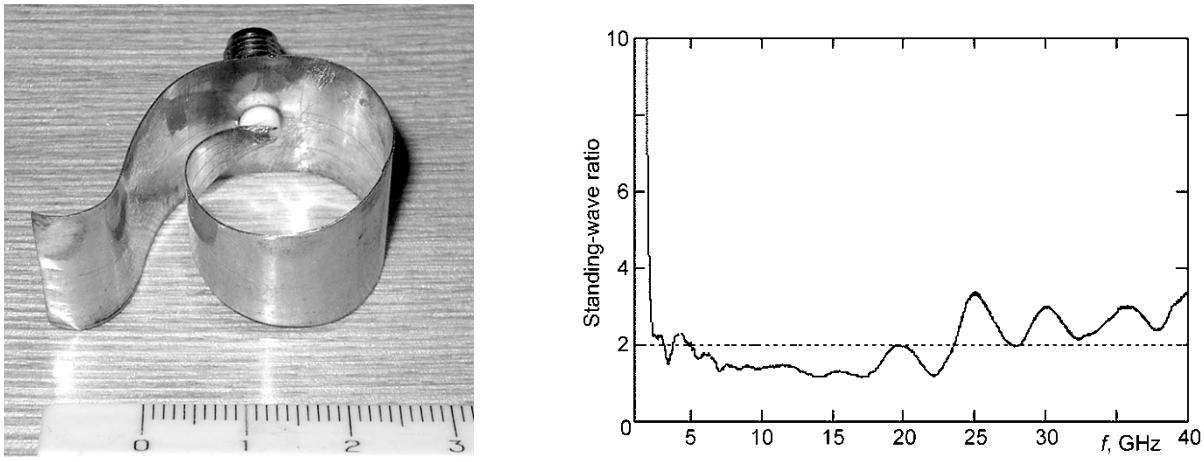

Fig. 2. UWB antenna-transmitter and its spectral characteristic.

Number of counts in the time window	16–4096
Jitter	1.5 ps + 0.0001%
Intrinsic noise level, RMS estimate	<2 mV
Amplitude channel capacity	12 bit
Measurement error, less than	1% of the measurable parameter

Model media of an oil-and-gas collector were investigated in open air with the use of a focusing system. Two identical UWB antennas-transmitters of special design (Fig. 2) were used as basic transmitting elements placed in the foci of the system. The antenna has small overall dimensions, stable phase center, linear polarization, cardioid directional pattern, and wide locking band.

The focusing system comprised two modified ellipsoid reflectors each included in the Cassegrain scheme (Fig. 3). This design allowed us to obtain a beam diameter of 3–5 cm in open air and hence to exclude the influence of side reflections.

The examined substance (the model medium) was placed in a cell with plane sides (Fig. 3). As the basic fraction of the model media, quartz sand was used, and oil extracted from well No. 418 of the Mirnoe field and from

TABLE 1

Serial number	Model medium	Water, %	Salinity, g/L	Clay, %	Sand, %	Oil, %	Gas (methane), %	Thickness, m
	Water–clay layer (well)	88	3	12	0	0	0	0.2
	Oil-bearing layer	6	17	0	85	9	0	5
	Gaseous capping layer	4,5	17	0	85	0	10.5	1
	Clay capping layer	3	17	97		0	0	2
	Water-bearing layer	15	17	0	85	0	0	3

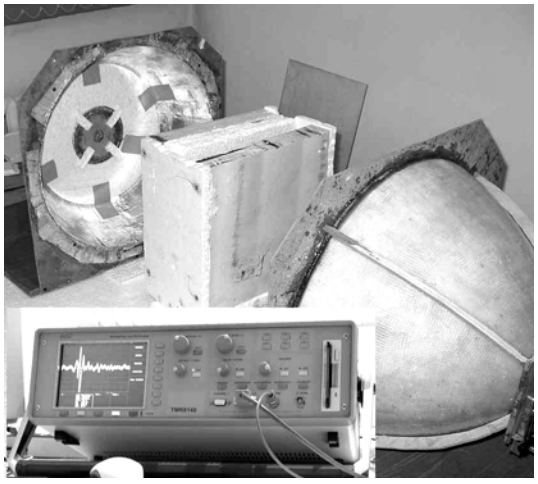

Fig. 3. Experimental setup.

well No. 11 of the Kazanskoe field of the Tomsk Region was used as a filling fraction. The salt solution was prepared from distilled water and common salt.

According to the well-known notion of the structure of oil-and-gas collector media [1, 2], it was assumed that the oil-bearing layer is bounded from above by gaseous and clay capping layers and from below by a water-bearing layer. The percentage of basic fractions in these media is tabulated in Table 1. It was assumed that radio-pulse probing should be carried out inside the oil-bearing layer, in particular, directly from a horizontal well filled with a water–clay solution.

The use of the collimated beam allowed us to estimate the transmissivity and reflectivity of UWB pulses for a concrete model medium by means of a comparison of incident, transmitted, and reflected pulse waveforms and then, with the use of a model describing the interaction between radiation and substance, to estimate the electrophysical parameters of the examined medium. The incident pulse waveform was fixed as a transmitted pulse waveform for the remote cell. Fig. 4 shows examples of waveforms of UWB pulses with duration of 100 ps in the case of probing of a sand layer and an oil-bearing layer with thickness $d = 50$ mm.

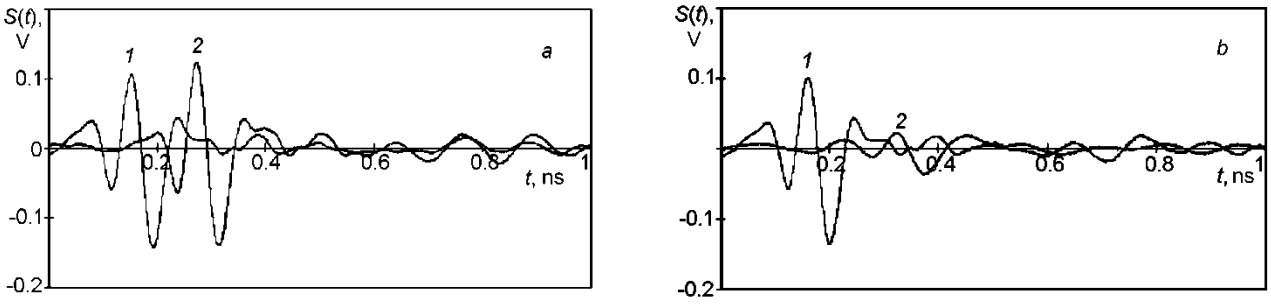

Fig. 4. Waveforms of UWB pulses in the case of probing of the empty cell (curve *1*) and the cell filled (curve *2*) with sand (*a*) and oil-bearing layer (*b*). The cell thickness was 50 mm.

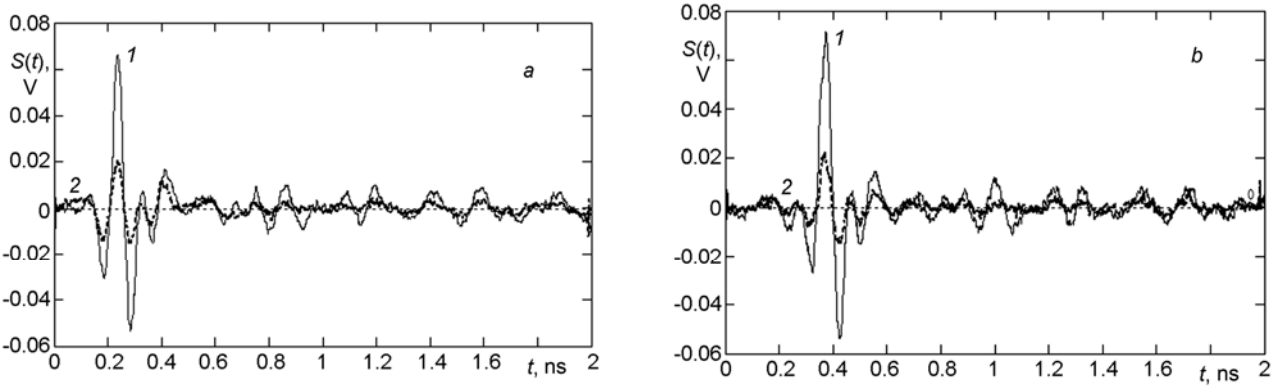

Fig. 5. Waveform of UWB pulses reflected from a metal screen (curve *1*) and system of layers (curve *2*) comprising oil- (11 mm) and water-bearing (34 mm) layers (*a*) as well as an oil-bearing layer (12 mm) and a gaseous capping layer (34 mm) (*b*).

To measure reflected pulses, a system was assembled that allowed us to measure the reflection coefficient of picosecond pulses for a two-layer model media comprising oil- and water-bearing layers or an oil-bearing layer and a gaseous capping layer. To this end, a signal was fed into the transmitting channel through a measuring tee taken from the kit of an R4-36 oscillograph with the operating frequency band 4–12 GHz. The reflected (object) signal was taken from the second arm of the tee. In this case, the direct losses were ≤ 4 dB, and the decoupling between transmitting and receiving channels was >30 dB. Figure 5 shows examples of measured UWB waveforms with duration of 100 ps reflected from the cell with different model media. The waveform of the probing (reference) pulse (curve *1*) was fixed as that of the pulse reflected from a metal screen placed immediately ahead of the layers.

We note that rather small thickness of model media was used in all our experiments. Use of actual thickness of oil-bearing and other layers presented in Table 1 is technically difficult. Transition to actual thickness is made theoretically.

From a comparison of Figs. 4 and 5 it can be seen that in the probing scheme, the structure of the media influences significantly the signal waveforms, while in the scheme with reflection, the first interface where the electrophysical properties undergo most significant changes gives the main contribution. Therefore, the signal reflected from the front oil-bearing layer dominates. This is physically justified. In this case, close similarity of the object (curve *2*) and reference signal waveforms (curve *1*) was retained. The correlation coefficient was close to 0.7. A comparison of the object signal with signals from the water-bearing and gaseous capping layers demonstrated their certain difference. However, without additional data processing, it is difficult to select signals reflected from the back layer boundaries,

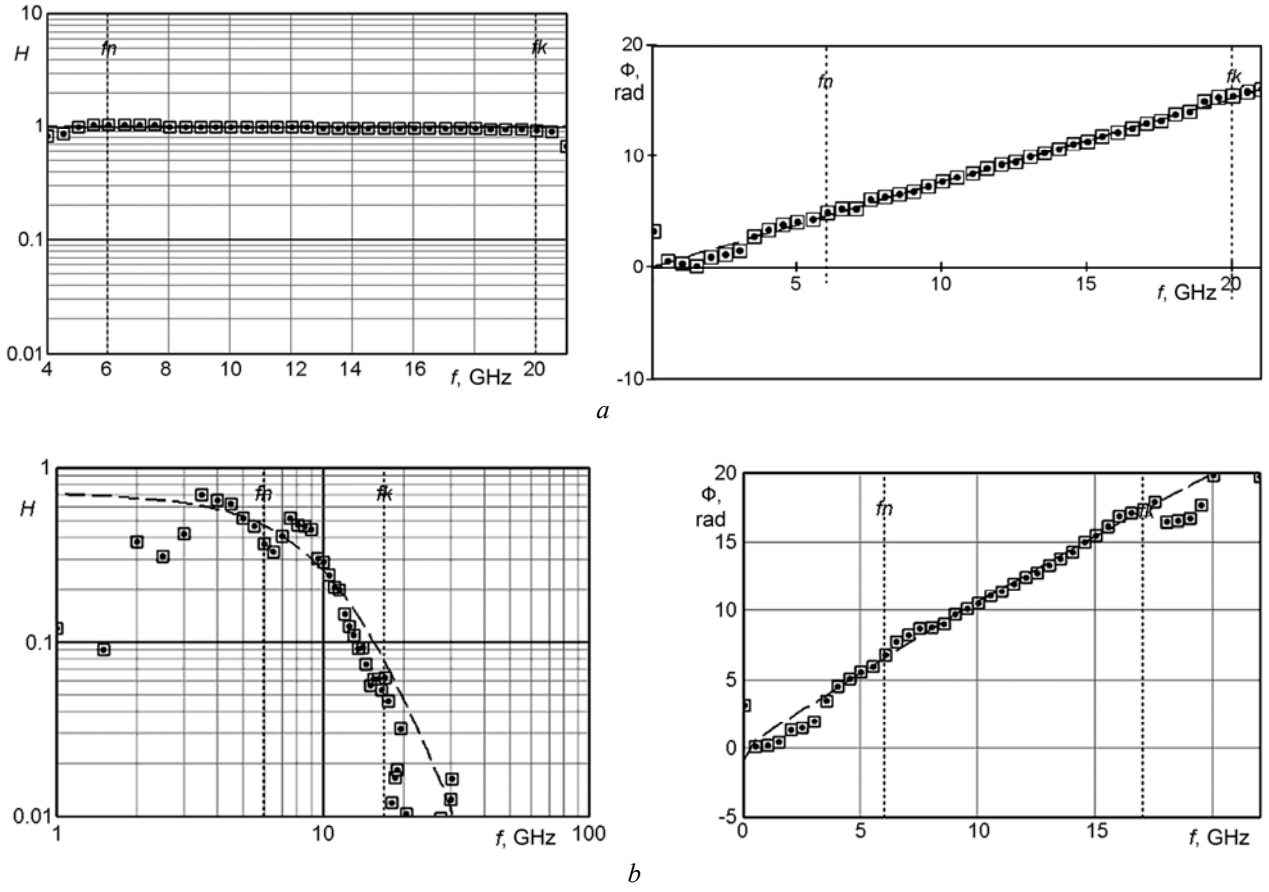

Fig. 6. Amplitude-frequency characteristic and phase spectrum of the transfer function of the plane quartz sand (*a*) and water-bearing layers (*b*).

which is explained by fast signal decay in the preceding absorbing layers. It is most easily to interpret data on probing of the layers. We consider these data as basic ones.

Calculations of the reference ($S_x(f)$) and object signal spectra ($S_y(f)$) allowed us to find the transfer function of the medium $W(f) = S_y(f)/S_x(f)$. As is well known, the shape of this function in the frequency range occupied by the sensing pulse $[fn, fk]$ must be independent of the signal waveform and must be determined only by the characteristics of the medium. Figure 6 shows examples of the amplitude-frequency characteristic (AFC) $H(f) = |W(f)|$ and phase spectrum $\Phi(f) = \arg\{W(f)\}$ for probing of quartz sand and water-bearing layers with thickness $d = 50$ mm by a 100-ps pulse. For samples of pure oil, the corresponding dependences were similar to those for dry sand, which demonstrates small water content in the oil. From the dependences obtained it can be seen that the oil-bearing medium, unlike the dry substance, possesses both absorption and scattering properties. It is obvious that these properties are caused by the presence of a certain amount of water in the oil-bearing medium.

The scattering properties of clear water have been investigated well enough [6, 7]; they are adequately described by the so-called modified Debye theory. This is confirmed by the experimental data on the dielectric permittivity of water $\varepsilon = n^2 = \varepsilon' + i\varepsilon''$ shown in Fig. 7. They were measured using an Agilent Vector Measuring Network Analyzer. Measurements were performed using the standard technique with the open end of the coaxial waveguide submerged into water. The solid curves superimposed on the experimental data were drawn with the use of the modified Debye theory. The theory and experiment coincide well both for clear and salty waters. It can be seen that

TABLE 2

Serial number	Medium	n	ε
1	Sand	1.72 ± 0.01	2.94 ± 0.02
2	Oil	1.46 ± 0.02	2.22 ± 0.04
3	Bentonite	2.07 ± 0.02	4.3 ± 0.1

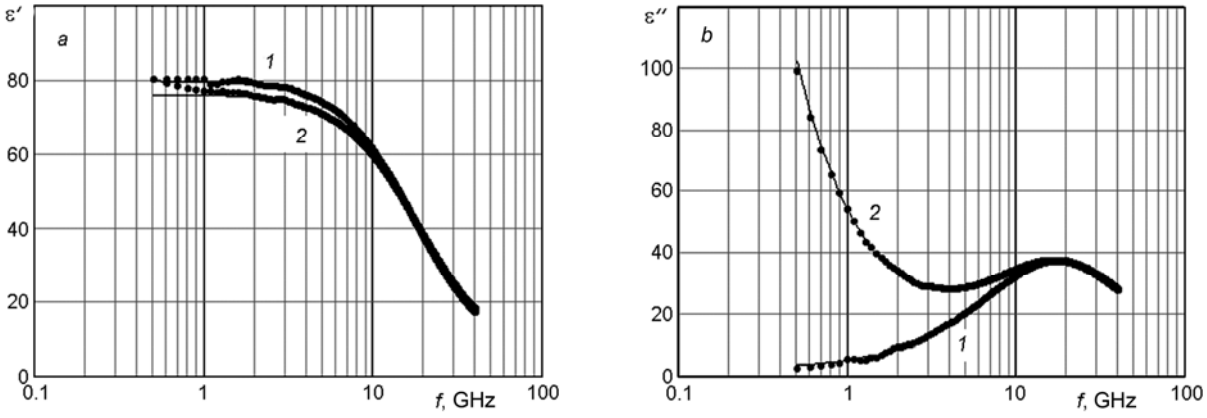

Fig. 7. Real (*a*) and imaginary parts (*b*) of the complex dielectric permittivity for clear (curve *1*) and salty waters ($s \approx 17$ ‰, curve *2*) at a temperature of 21°C.

the scattering properties of water are most clearly pronounced in the range of frequencies occupied by the 100-ps UWB pulse, that is, at $f = 1 - 20$ GHz .

THEORETICAL ANALYSIS

To describe the transfer function $W(f)$ for probing of a plane layer with thickness d and complex refractive index n, we now take advantage of the well-known formula [8]

$$W(f) = \frac{4n}{(n+1)^2 - (n-1)^2 \exp\{2iknd\}} \exp\{ikd(n-1)\} .$$

Here $k = 2\pi f / c$ is the wave number for free space. The exponent in the denominator of this expression describes multiple re-reflections inside of the layer. As the absorption in the medium increases, the role of these re-reflections noticeably decreases.

The above formula allows the refractive index n and dielectric permittivity $\varepsilon = n^2$ of the main fractions of media of the oil-and-gas collector that do not contain water to be estimated by means of approximation of the available experimental data by the least square method (Table 2). The refractive index of bentonite (clay) was taken from [9].

The parameters of the main fractions so obtained can be used to calculate the parameters of mixtures for the so-called refraction model [9] according to which

$$n = \sum_j n_j w_j ,$$

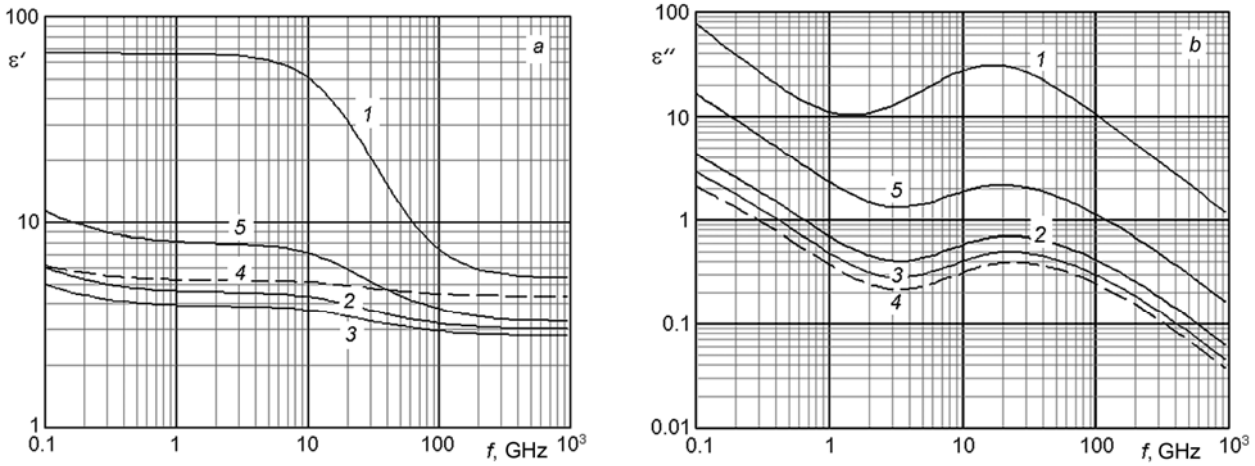

Fig. 8. Real (*a*) and imaginary components (*b*) of the dielectric permittivity of media of the oil-and-gas collector. Here curve *1* is for a water-clay layer (well), curve *2* is for an oil-bearing layer, curve *3* is for a gaseous capping layer, curve *4* is for a clay capping layer, and curve *5* is for a water-bearing layer.

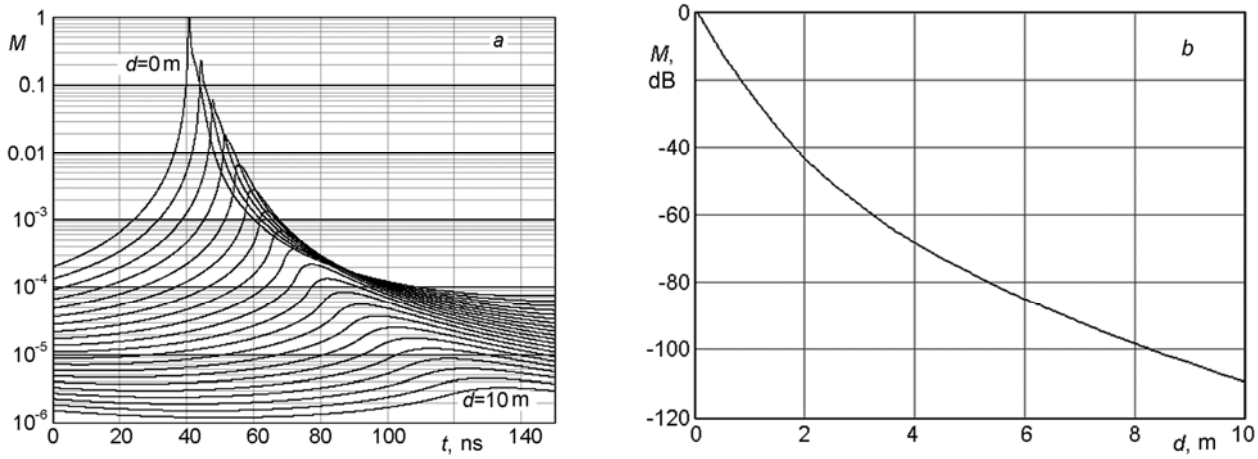

Fig. 9. Waveform of the UWB-pulse envelope (*a*) and decay of its maximum (*b*) versus the depth of penetration into the oil-bearing layer.

where w_j is the relative volume content of the *j*th component with the complex refractive index n_j. The dashed curve in Fig. 6*b* shows the approximation of the transfer function of the oil-bearing layer with allowance for the scattering properties of water, which confirms once again the applicability of the refraction formula. Figure 8 shows values of the dielectric permittivity of the main media of the oil-and-gas collector obtained by the above-described method and extrapolated toward the frequency range 0.1–1000 GHz at a temperature of 21°C.

The spectra of the complex dielectric permittivity of mixtures so obtained can be used to estimate the transmission and reflection of any arbitrary pulses for simple layers and their arbitrary combinations. Figure 9 shows the calculated radiation pulse decay versus the depth of penetration into a simple oil-bearing layer. The signal envelope (amplitude) is meant the modulus of the corresponding analytical signal. In our calculations, we used the so-called balanced optimal pulsed signal for which [10]

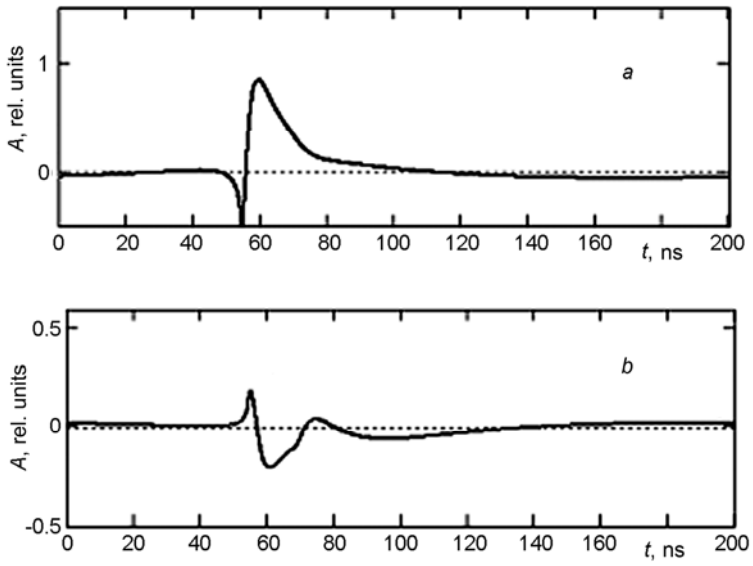

Fig. 10. Waveforms of pulses reflected from a 1-m oil-bearing layer after WDM processing in the case of probing up (*a*) and down (*b*) of the oil-and-gas collector.

$$S_x(t) = S_0\left(\frac{t}{T}\right)^p \left\{\exp\left(-\frac{t}{T}\right) - m^{p+1}\exp\left(-m\frac{t}{T}\right)\right\}, \quad t \ge 0\,,\ T_0 = T\frac{p+1}{m-1}\ln(m)\,.$$

Here T_0 is the duration of the first (short) pulse lobe at zero level. We set $T_0 = 1$ ns and $p = m = 6$. It can be seen that losses per unit length in the process of penetration into the oil-bearing layer decrease smoothly from 25 dB/m at the surface to 5 dB/m at a depth of 10 m. The reason is fast absorption of high-frequency signal components and slower absorption of low-frequency components with depth.

In the case of radar probing of the oil-and-gas collector directly from a horizontal well, the well boundary where the water-clay layer is transformed into the oil-bearing one has the greatest influence on the wave reflection. In this case, the total reflected signal comprises two components $S(t) = Y(t) + y(t)$, first of which considerably exceeds the second caused by reflections from deep layers. The modulus of this function can be estimated as

$$|S(t)| = \sqrt{[Y(t) + y(t)]^2} \approx |Y(t)|\left\{1 + \frac{y(t)}{|Y(t)|}\right\}.$$

From here we obtain the simple estimate of the normalized weak signal

$$A(t) = \frac{y(t)}{|Y(t)|} \approx \frac{|S(t)|}{|Y(t)|} - 1\,.$$

We call this method the weighed-differential method (WDM) of separating weak signals from deep layers. It is important that the suggested method allows the difference in signals for probing down and up from a horizontal well to be clearly distinguished (Fig. 10). This is especially important for navigation of drilling tools and tomographic reconstruction of the 3D-structure of media of the oil-and-gas collector.

CONCLUSIONS

Our experimental and theoretical studies on UWB sensing of model media of the oil-and-gas collector have allowed us to reveal the basic laws of radiation pulse propagation through plane-layered media surrounding wells and to develop the new method of weighed-differential processing of probing UWB signals for radio-pulse logging and navigation of drilling tools under conditions of horizontal wells. Finally, the result obtained gives the positive answer to the question whether or not the UWB methods are efficient for radio pulse logging in exploitation of hydrocarbon fields.

REFERENCES

1. M. I. Épov, G. M. Morozova and E. Yu. Antonov, Electromagnetic Flaw Detection in Casing Strings of Oil–and–Gas Wells. Fundamentals of Theory and Technology [in Russian], GEO Affiliate of the Publishing House of the Siberian Branch of the Russian Academy of Sciences (2002).
2. M. I. Épov and V. N. Glinskikh, Electromagnetic Logging: Modeling and Inversion [in Russian], GEO Academic Publishing House, Novosibirsk (2005).
3. V. G. Sugak, A. V. Bukin, O. A. Ovchinkin, Yu. A. Pedenko, and Yu. S. Silaev, Nauka Innov., **1**, No. 2, 32–43 (2005).
4. V. B. Boltintsev, Construction of a structural model of natural–technical objects from the data of electromagnetic ultrawideband probing, Author's Abstract of Cand. Tech. Sci. Dissert., Krasnoyarsk (2006).
5. R. R. Zinnatullin, Experimental research and comparative analysis of electrophysical and filtration characteristics of oil disperse systems, Author's Abstract of Cand. Tech. Sci. Dissert., Ufa (2006).
6. F. T. Ulaby, R. K. Moore, and A. K. Fung, Microwave Remote Sensing. Active and Passive, Addison–Wesley Public. Comp., London (1981).
7. A. Poison, IEEE J. Ocean Eng., No. 1, 41–50 (1980).
8. L. M. Brekhovskikh, Waves in Layered Media [in Russian], Nauka, Moscow (1973).
9. S. A. Komarov and V. L. Mironov, Microwave Sensing of Soils [in Russian], Scientific–Publishing Center of the Siberian Branch of the Russian Academy of Sciences, Novosibirsk (2000).
10. F. M. Stadnik and G. V. Ermakov, Radiotekh. Elektron., **40**, No. 7, 1009–1016 (1995).